

## QUANTUM COMPUTING WITH ELECTRONS FLOATING ON LIQUID HELIUM

M.I. Dykman

*Department of Physics & Astronomy, Michigan State University  
East Lansing, MI 48824, USA*

P.M. Platzman

*Bell Laboratories, Lucent Technologies  
Murray Hill, NJ 07974, USA*

Electrons on a helium surface form a quasi two-dimensional system which displays the highest mobility reached in condensed matter physics. We propose to use this system as a set of interacting quantum bits. We will briefly describe the system and discuss how the qubits can be addressed and manipulated. The working frequency of the proposed quantum computer is  $\sim 1$  GHz. Careful analysis shows that the relaxation rate can be at least 5 orders of magnitude smaller, for low temperatures.

### 1. Introduction

Finding physical systems that are suitable for quantum computation is a major challenge, since these systems must consist of a large number of quantum objects whose states and interactions can be conveniently manipulated. In addition, the qubits must be sufficiently isolated from other degrees of freedom so that they do not disturb the time dependence of the computational wave function. It should also be possible to read out the final state of the system (the result of the calculation)[1]. Ions and neutral atoms in traps [2], cavity quantum electrodynamic systems [3], bulk NMR systems[4], quantum dots[5], nuclear spins of atoms in doped silicon devices [6], localized electron spins in semiconductor heterostructures[7], and Josephson-junction based systems[8] have been proposed, and in a number of cases proof of the principle has been convincingly demonstrated. Many of these suggestions and some very recent ideas are discussed in these Proceedings. However, for all proposed systems there are high technological and scientific barriers, which must be overcome to achieve a useful quantum computer.

We believe, based on realistic estimates[9], that there already exists a system that is a good candidate for a scalable analog quantum computer (AQC) with an easily manipulated set of qubits. This is a system of electrons floating on the surface of superfluid helium. It is incredibly clean, because the electrons essentially reside in vacuum, and the closest condensed matter is the superfluid helium, which is itself very pure, with a microscopically smooth surface. Electrons on helium display the highest mobility achieved in a condensed matter system so far[10]. They have been extensively studied theoretically and experimentally[11], and are by now well understood. Our estimates indicate [9] that, under realistically obtainable geometry, temperature, and magnetic field, the electrons can function as qubits provided they

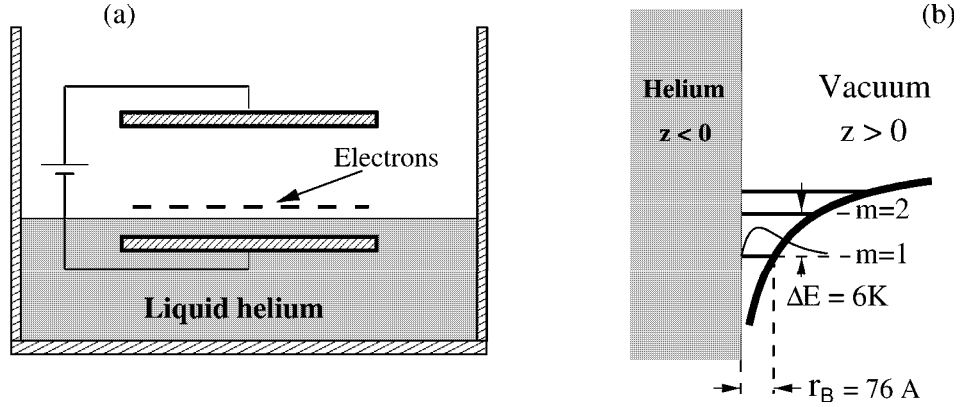


Fig. 1. (a) Conventional geometry of experiments on electrons trapped at the helium-vacuum interface. The electrons are attracted to the liquid helium by the image potential and an electrostatic potential of the capacitor, and are free to move in the plane. (b) The hydrogenic energy levels for electron motion in the  $z$  direction transverse to the helium surface, along with a typical  $m = 1$  ground state wave function are displayed in the image potential for  $z > 0$ .

are confined by micron-size electrodes located below the helium surface.

The system of electrons on helium has several important advantageous features. First of all, different states of a qubit have different electric dipole moments. This makes it relatively simple to address the qubits and to read out their states. A realistic calculation shows that the coherence time of the electron states is  $\sim 10^5$  times the reciprocal working frequency of the proposed AQC, which is determined by the Rabi frequency and the energy of qubit-qubit interaction. The typical interqubit distance is  $\sim 1 \mu\text{m}$ , and therefore fabricating a multi-qubit system should not require technological breakthroughs.

In what follows we briefly review the physics of electrons on helium, describe the proposed design of the quantum computer [9], and discuss how operations on qubits can be performed.

## 2. Electrons on helium

The geometry of experiments on electrons trapped above the liquid-helium surface is shown schematically in Fig. 1. This very clean system has been recognized as a perfect tool for investigating many basic concepts of condensed matter physics. Not only the electron energy spectrum and scattering mechanisms are well established[11], but this is one of only a few well-understood strongly correlated electron systems. Correlation effects are strong because, although the system is nondegenerate, the ratio of the Coulomb energy of the electron-electron interaction to the thermal energy  $\Gamma = e^2(\pi n_e)^{1/2}/k_B T$  usually exceeds 20 ( $n_e$  is the electron density; typically  $n_e \sim 10^8 \text{ cm}^{-2}$ ). For  $\Gamma > 130$ , the electrons form a Wigner crystal[12, 13], whereas for higher temperatures they form a nondegenerate correlated electron liquid, with unusual transport characteristics [14].

An electron on a bulk helium film is bound in the direction  $z$  normal to the helium surface by an image potential of the form  $V(z) = -\Lambda e^2/z$  (see Fig. 1), with  $\Lambda = (\epsilon - 1)/4(\epsilon + 1)$  ( $\epsilon = 1.057$  is the dielectric constant of liquid helium). Because there is a barrier of  $\approx 1$  eV for penetration into the helium, the electron  $z$ -motion is described by a 1D hydrogenic spectrum. The  $m$ th state has an energy  $E_m = -R/m^2$ , with an effective Rydberg energy

$R = \Lambda^2 e^4 m_e / 2\hbar^2 \approx 8$  K, and effective Bohr radius  $r_B = \hbar^2 / \Lambda m_e e^2 \approx 76$  Å (Fig. 1).

Electronic transitions between the states in Fig. 1b were observed using microwave spectroscopy[15]. The level spacing could be controlled by a static electric field  $\mathcal{E}_\perp$  normal to the helium surface from the capacitor in Fig. 1a. This field Stark-shifted the transition frequencies. The linear Stark shift is  $\approx 1$  GHz/(V/cm), which will be important for our AQC. The calculated shift was in excellent agreement with the experiment. For  $T = 0.4$  K the natural linewidth for the  $1 \rightarrow 2$  phototransition was estimated from measurements of inhomogeneously-broadened spectra to be below 15 MHz[16].

For  $T < 0.7$  K, the only substantial electron coupling to the outside world leading to decoherence effects is to thermally excited height variations  $\delta(\mathbf{r}, t)$  of the helium surface, where  $\mathbf{r}$  is the electron in-plane coordinate. These variations are described as propagating capillary waves, riplons. Riplons are very soft excitations: for the wave vectors  $k < 5 \times 10^5$  cm<sup>-1</sup>, which are of interest for the AQC, the ripplon energies are  $\hbar\omega_r(\mathbf{k}) < 4 \times 10^{-3}$  K. Therefore, at  $10^{-2}$  K many such riplons are present, and the corresponding root-mean-square displacement  $\delta_T$  of the surface is determined by thermal fluctuations, with  $\delta_T \approx 2 \times 10^{-9}$  cm.

The electron-riplon coupling energy is

$$H_{e-r} = e\hat{\mathcal{E}}_\perp\delta(\mathbf{r}, t), \quad (1)$$

where  $\hat{\mathcal{E}}_\perp$  is the effective  $z$ -directed electric field on the electron. It is given by the sum of the externally applied field  $\mathcal{E}_\perp$  and the [nonlocal in  $\mathbf{r}$ ] field from the image potential  $\sim 10^2 - 10^3$  V/cm.

In the lowest hydrogenic level it is the weak coupling to riplons which limits the in-plane mobility of the surface state electrons. It also determines the dephasing rate of the  $m \rightarrow m'$  photoinduced transitions for unconfined electrons. This dephasing rate is of the order of the intraband momentum relaxation rate  $\tau^{-1}$ . In the single-electron approximation,  $\tau^{-1} = e^2 \mathcal{E}_{\text{eff}}^2 / 4\sigma\hbar$ , where  $\mathcal{E}_{\text{eff}}$  is the known characteristic value of the field pressing the electron to the surface (it is linear in  $\mathcal{E}_\perp$ ), and  $\sigma$  is the surface tension of helium. This expression is in good agreement with the measurements [17]. The relaxation rate is record low: from the recent mobility measurements[10],  $\tau^{-1} \approx 10^7$  s<sup>-1</sup>, in agreement with the upper bound on the photoabsorption linewidth cited before.

Since all measurements refer to a strongly correlated electron system, one may ask if the agreement of the single-electron theory and experiment is not fortuitous. However, in a broad range of  $T$  and  $n_e$ , the single-electron transport theory is essentially applicable in the absence of a magnetic field [14]. This is no longer true in the presence of a field  $B_\perp$  normal to the electron layer, which is also of interest for the AQC. It turns out that transport in the correlated electron system can be analyzed in a non-perturbative way[14]. The many-electron conductivity displays a specific dependence on the parameters of the system, and in particular, it is a non-monotonic function of  $B_\perp$ . The theory is in full agreement with the experiment[18], which reassures one that our understanding of the electron system on helium is adequate.

Besides intraband relaxation, the coupling to riplons gives rise to transitions from the excited  $m = 2$  to the ground  $m = 1$  hydrogenic band in Fig. 1. A simple estimate for the interaction (1) gives the relaxation rate  $T_1^{-1} \sim (R/\hbar)(\delta_T/r_B)^2$ . Since  $\delta_T/r_B \sim 10^{-3}$ , the rate  $T_1^{-1}$  is  $\sim 10^{-6}$  of the transition frequency  $\sim 120$  GHz. This suggests using the lowest two hydrogenic levels of an individual electron as a convenient qubit, whose state can be changed by the application of a resonant microwave field.

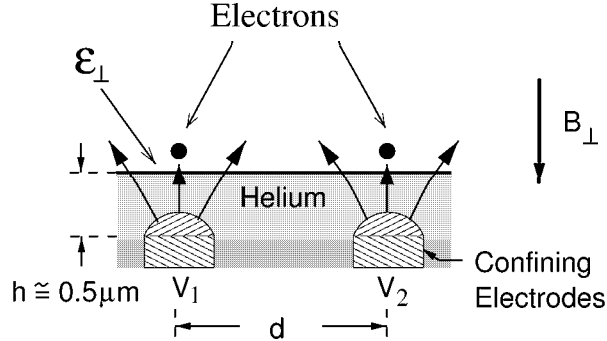


Fig. 2. Electrons on helium above a patterned substrate. The rough dimensions ( $h \approx d$ ), the field lines, and the gate voltages are included. The average distances of the electron from the helium surface in the hydrogenic states  $|1\rangle$  and  $|2\rangle$  are  $\approx 11$  nm and  $\approx 45$  nm, respectively, for small pressing field  $\mathcal{E}_\perp$ .

For a field amplitude  $E_{\text{RF}} = 1$  V/cm, the Rabi frequency  $\Omega = |eE_{\text{RF}}\langle 1|z|2\rangle|/\hbar \sim eE_{\text{RF}}r_B/\hbar$  of the oscillations of a resonantly driven electron between the lowest and the first excited state is about  $10^9$  s $^{-1}$ . This is the working frequency of the quantum qubit we are suggesting. Even a laterally unconfined electron has  $\Omega T_1 > 10^4$ .

### 3. Qubits using electrons on helium

Recently we suggested[9] that electrons on helium can be used as addressable qubits if they are confined laterally. The geometry is shown schematically in Fig. 2. The lower plate of the capacitor that holds electrons at the helium surface is patterned and forms a set of individually addressable micro electrodes. To make the frequency of resonant energy exchange between neighboring electrons of the order of  $\Omega \sim 10^9$  s $^{-1}$ , the distance  $d$  between the dots should be  $\sim 0.5$   $\mu\text{m}$ . Consequently, the electrodes should be submerged at  $h \sim d \sim 0.5$   $\mu\text{m}$  beneath the helium surface. This geometry allows accommodation of  $\geq 10^8$  qubits, for a typical area of the helium surface 1 cm $^2$ .

The electrode potentials  $V_n$  create both out-of-plane and in-plane fields on the electrons. They can be easily found for a spherical electrode of radius  $R$ . If the center of the sphere is at the distance  $h$  below the surface, the  $V_n$ -dependent part of the pressing field  $\mathcal{E}_\perp$  is  $\mathcal{E}_n \approx V_n R/h^2$ . Then, for the geometry in Fig. 2, the change of the Bohr frequency of the  $1 \rightarrow 2$  transition by 1 GHz should occur for the increment  $\Delta V_n \sim 0.1 - 1$  mV [with account taken of the neutralizing background]. This allows one to make a **one-qubit gate** by tuning the Bohr frequency of the targeted electron to the frequency of the externally applied microwave radiation. Depending on the duration of the radiation pulse  $T_{\text{RF}}$  with respect to the Rabi frequency  $\Omega$ , the qubit will be put into an arbitrary superposition of the ground and excited states. In fact, an optimal arrangement is to combine a radiation pulse with the pulse of the control voltage  $V_n$ , which tunes the qubit into resonance for a desired amount of time.

Electron confinement gives rise to a further dramatic increase of the lifetime of the excited state  $T_1$ , and makes the coherence time  $T_2$  very large. The spectrum of a single pinned electron consists of a ladder of discrete in-plane energy levels connected with the ground and excited hydrogenic states in Fig. 1. The level spacing  $\hbar\Omega_\parallel$  can be estimated for spherical electrodes, in which case  $m\Omega_\parallel^2 \approx e^2 R(h^2 - R^2)^{-2} + eRV_n h^{-3}$ . This spacing is not commensurate with

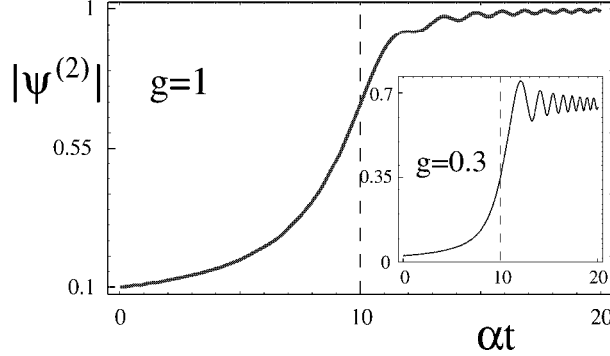


Fig. 3. Excitation transfer between the qubits 1 and 2, which are initially ( $t < 0$ ) in the excited and ground states, respectively. The Bohr frequencies of the qubits are linearly changed in time,  $\Omega_{1,2}(t) = \Omega_{1,2}(0) \mp \alpha t$  and become equal to each other for  $\alpha t = 10$ . Solid curves show the amplitude of the excited state of the qubit 2 for different effective coupling parameters  $g = \Omega_{sw}/\alpha^{1/2}$ .

$E_2 - E_1$ . Therefore a transition from the state  $m = 2$  requires emission of a ripplon with energy  $\sim \hbar\Omega_{\parallel}$ , which is much higher ( $\sim 0.4$  K) than  $\hbar\omega_r$ . We can further suppress one-ripplon decay processes if we apply a magnetic field  $B_{\perp}$  normal to the electron layer. It will open up gaps  $\hbar e B_{\perp}/mc$  in the in-plane excitation spectrum, which are  $\approx 2$  K for  $B_{\perp} = 1.5$  T.

The dephasing rate  $T_2^{-1}$  of a confined electron is determined by a kind of quasi-elastic scattering of thermally excited riplons, which is similar to the single-electron dephasing rate in quantizing magnetic fields[19]. It contains a factor  $(\delta_T/r_B)^4 \sim 10^{-11}$  and is estimated[9] to be  $T_2^{-1} < 10^4$  s $^{-1}$  for  $T = 10$  mK. The ratio of the working frequency to the relaxation rate is  $\Omega T_2 > 10^5$ . Other sources of noise and fluctuations can be reduced to the level where they give an even smaller dephasing rate[9].

**Two-qubit gates** are often discussed in terms of pairing qubits in turn, in isolation from the rest of the system, and manipulating them in a few fundamental ways. However, in real physical systems interactions are not easily turned on and off. Therefore we would argue that the manipulation of interactions in the whole interacting many qubit system, and the final measurement or collapse of the wave function must be thought of as part of the ultimate computation process. In our computer the qubit-qubit interactions come from the charge on the electrons and are always there. The important ones, as regards the  $z$ -motion, are dipolar with energy given by  $\sum_{n \neq m} e^2 z_n z_m / 2d_{nm}^3$ , where  $d_{nm}$  is the distance between the  $n$ th and  $m$ th electrons.

The interelectron coupling allows us to perform both CNOT and swap operations. The latter can be done by sweeping the Bohr frequencies  $\Omega_n = [E_2^{(n)} - E_1^{(n)}]/\hbar$  of the electrons past each other, as a result of the voltage change on the underlying electrodes. At resonance, an excitation will be transferred between nearest neighbors over the time  $\sim \Omega_{sw}^{-1}$ ,  $\Omega_{sw} = e^2 | \langle 1|z|2 \rangle |^2 / \hbar d^3$ . For the parameters in Fig. 2, this time is  $10^{-9}$  s.

Kinetics of excitation transfer between two qubits for linear change of the electrode potentials  $V_{1,2}$  is illustrated in Fig. 3. The amplitude of the initially occupied excited state of the qubit 1 approaches  $\exp(-\pi g^2)$  for large time. Therefore, by adjusting the rate of the potential change, excitation transfer can be made exponentially efficient.

A simple way of measuring the state of a qubit is to apply a pulse of a negative voltage to the underlying electrode. The electron may then tunnel away from the surface. For the

geometry in Fig. 1, the tunneling was investigated before[11, 20]. The tunneling rate is exponentially larger if the electron is in the excited rather than the ground state. This allows one to detect the electron state[9]. Alternatively, the electron states may be detected by attaching single electron transistors to the control electrodes.

The system of two-dimensional electrons on helium is unique in the context of large AQC systems. It is scalable, easily manipulated, and has perfectly acceptable decoherence times. It has been carefully investigated theoretically and experimentally, and there seems to be no existing technological barriers present for making an AQC using it.

### Acknowledgments

MID acknowledges support from the NSF through grant No. ITR-0085922.

1. D.P. DiVincenzo, *Science* **269**, 255 (1995); D.P. DiVincenzo and D. Loss, *Superlattices and Microstructures* **23**, 419 (1998).
2. J.I. Cirac and P. Zoller, *Phys. Rev. Lett.* **74**, 4091 (1995); C. Monroe *et al.*, *Phys. Rev. Lett.* **75**, 4011 (1995); B.E. King *et al.*, *Phys. Rev. Lett.* **81**, 1525 (1998); Q.A. Turchette *et al.*, *Phys. Rev. Lett.* **81**, 3631 (1998).
3. Q.A. Turchette *et al.*, *Phys. Rev. Lett.* **75**, 4710 (1995);
4. N.A. Gershenfeld and I.L. Chuang, *Science* **275**, 350 (1997); D.G. Cory, M.D. Price, and T.F. Havel, *Physica D* **120**, 82 (1998); I.L. Chuang *et al.*, *Phys. Rev. Lett.* **80**, 3408 (1998); I.L. Chuang *et al.*, *Nature* **393**, 143 (1998).
5. D. Loss and D.P. DiVincenzo, *Phys. Rev. A* **57**, 120 (1998); J.A. Gupta *et al.*, *Phys. Rev. A* **59**, R10421 (1999); M.S. Sherwin, A. Imamoglu, and Th. Montroy, *Phys. Rev. A* **60**, 3508 (1999); A. Imamoglu *et al.*, *Phys. Rev. Lett.* **83**, 4204 (1999).
6. B.E. Kane, *Nature* **393**, 133 (1998).
7. R. Vrijen *et al.*, *Phys. Rev. A* **62**, 012306 (2000).
8. V.D. Averin, *Solid State Commun.* **105**, 659 (1998); Yu. Makhlin, G. Schön, and A. Shnirman, *Nature* **398**, 305 (1999); L.B. Ioffe *et al.*, *Nature* **398**, 679 (1999); Y. Nakamura *et al.* *Nature* **398**, 786 (1999).
9. P.M. Platzman and M.I. Dykman, *Science* **284**, 1967, (1999); M.I. Dykman and P.M. Platzman, *Fortschr. Phys.* **48**, 1095 (2000).
10. K. Shirahama, S. Ito, H. Suto, and K. Kono, *J. Low Temp. Phys.* **101**, pp. 439-44 (1995).
11. "Two dimensional electron systems on helium and other cryogenic substrates", ed. E.Y. Andrei (Kluwer, NY 1997).
12. C.C. Grimes and G. Adams, *Phys. Rev. Lett.* **42**, 795 (1979).
13. D.S. Fisher, B.I. Halperin, and P.M. Platzman, *Phys. Rev. Lett.* **42**, 798 (1979).
14. M.I. Dykman, M.J. Lea, P. Fozooni, and J. Frost, *Phys. Rev. Lett.* **70**, 3975 (1993).
15. C.C. Grimes *et al.*, *Phys. Rev. B* **13**, 140 (1976).
16. A.P. Volodin and V.S. Edelman, *Sov. Phys. JETP* **54**, 198 (1981).
17. R. Mehrotra *et al.*, *Phys. Rev. B* **29**, 5239 (1984); A.J. Dahm and W.F. Vinen, *Physics Today* **40**, 43 (1987).
18. M.J. Lea *et al.* *Phys. Rev. B* **55**, 16280 (1997); M.J. Lea and M.I. Dykman, *Physica B* **251**, 628 (1998); E. Teske *et al.*, *Phys. Rev. Lett.* **82**, 2772 (1999).
19. M.I. Dykman, *Phys. Stat. Sol. (b)* **88**, 463 (1978).
20. G.F. Saville, J.M. Goodkind, and P.M. Platzman, *Phys. Rev. Lett.* **70**, 1517 (1993).